Mathematical Modelling and Analysis
Volume 29, Issue 1, 1–22, 2024
https://doi.org/10.3846/mma.2024.16979

Implicit Extended Discontinuous Galerkin Scheme for Solving Singularly Perturbed Burgers' Equations

Samaneh Khodayari-Samghabadi, Maryam Mondanizadeh and Sayed Hodjatollah Momeni-Masuleh

Department of Mathematics, Shahed University
P.O. Box 18151-159, Tehran, Iran
E-mail: samaneh.khodayari@gmail.com
E-mail: mondanizade1395@gmail.com
E-mail(*corresp.*): momeni@shahed.ac.ir

Received May 16, 2022; accepted January 12, 2024

Abstract. We present the implicit-modal discontinuous Galerkin scheme for solving the coupled viscous and singularly perturbed Burgers' equations. This scheme overcomes overshoot and undershoots phenomena in the singularly perturbed Burgers' equations. We present the stability analysis and obtain suitable ranges for penalty terms and time steps. Also, we gain the constant of trace inequality for the approximate function and its first derivatives based on Legendre basis functions. The numerical results have good agreement with the analytical and available approximate solutions.

Keywords: discontinuous Galerkin method, backward Euler method, viscous Burgers' equation, singularly perturbed Burgers' equation, stability analysis.

AMS Subject Classification: 65M60; 35K67; 35K15.

1 Introduction

The coupled non-linear system of the viscous Burgers' equation has applications to non-linear acoustics, shock wave traveling in the viscous fluid, in oil reservoir simulation. To approximate the viscous coupled Burgers' equations, Khater et al. [11] used the Chebyshev spectral collocation method and Runge-Kutta method of order four for spatial and temporal discretization, respectively.

Fourier pseudospectral method is employed by Rashid and Ismail [21] for solving viscous coupled Burgers' equation. Mittal and Arora [17] approximated the solution of a coupled system of viscous Burgers' equations with the cubic B-spline collocation scheme on the uniform mesh points for space and Crank-Nicolson formulation for time discretization. Mittal and Jiwari [18] used the polynomial differential quadrature and fourth-order Runge-Kutta methods for space and time discretization, respectively, and obtained numerical solutions of non-linear Burgers'-type equations. Doha et al. [8] combined the Jacobi-Gauss-Lobatto collocation method with the implicit Runge-Kutta (-Nyström) to solve the viscous coupled Burgers' equations accurately. Lai and Ma [15] and Li et al. [16] presented different lattice Boltzmann methods for solving the coupled viscous Burgers' equations. Bakodah et al. [5] approximate the solution of Burgers' equation with the modified Adomian decomposition method. Baccouch and Kaddeche [3] applied the Chebyshev collocation method for spatial discretization in one and two dimensions and the fourth-order Runge-Kutta method for temporal discretization. Alderremyet et al. [2] show that the variational iteration method has faster convergence than Laplace transform Adomian decomposition and Laplace transform homotopy perturbation methods for solving non-linear Burgers' equation.

The viscous coupled Burgers' equations involve non-linear propagation effects and diffusive effects. When the diffusion term approaches zero, the viscous coupled Burgers' equations become the inviscid coupled Burgers' equations, known as a singularly perturbed convection-diffusion problem. Laforgue and O'Malley Jr [14] applied exponential asymptotics to solve the singularly perturbed Burgers' equation. Bause and Schwegler [7] used a higher order finite element approximation with streamlined upwind Petrov-Galerkin, to reduce fake oscillations and anisotropic shock-capturing stabilization, to reduce over- and undershoots for solving systems of coupled convection-dominated transport equations. Uzunca [25] employed the adaptive discontinuous method for spatial discretization and the backward Euler method for temporal discretization to solve non-linear singularly perturbed advection-diffusion problems. Gowrisankar and Natesan [9] linearized singularly perturbed Burgers' equation using Newton's quasilinearization process and obtained a sequence of the convection-diffusion Burgers' equation. They solved the linear equations using the finite difference and upwind technique for spatial discretization and the backward Euler method for time discretization.

In this paper, we consider the coupled viscous and singularly perturbed Burgers' equations and apply the implicit discontinuous Galerkin (IDG) and implicit extended discontinuous Galerkin (IEDG) schemes to solve them. The accuracy of the proposed scheme is demonstrated and compared with other results given in the literature. If one uses the modal (or nodal) DG method for solving singularly perturbed Burgers' equation, the overshoot and undershoot phenomena occur in numerical results by passing the time. Usually, limiters are used to overcome this phenomena [13, 24]. To solve these phenomena, we extended the discontinuous Galerkin method to overcome them without using limiters. We numerically study the performance properties of the scheme with small diffusion terms. The numerical results are a good agreement with the

exact solution. We prove the stability of IDG and IEDG schemes and find the suitable ranges of penalty terms (to be stable) and time steps (to guarantee convergence). In the stability analysis, we compute the value of constants in trace inequality for a function and its derivatives. We use the Legendre polynomials as basis functions and the idea in [12]. The constants of trace inequalities, just for function, are achieved using orthogonal polynomials by Warburton and Hesthaven [26].

2 Problem formulation

Let $\Omega = [a, b]$ be a bounded domain in $\mathbb{R}$ with Lipschitz boundary $\partial\Omega$. Consider the following model of the coupled non-linear system of the viscous Burgers' equations:

$$\begin{pmatrix} \frac{\partial u}{\partial t} \\ \frac{\partial v}{\partial t} \end{pmatrix} - \epsilon \begin{pmatrix} \frac{\partial^2 u}{\partial x^2} \\ \frac{\partial^2 v}{\partial x^2} \end{pmatrix} + \begin{pmatrix} \eta u + \alpha v & \alpha u \\ \beta v & \xi v + \beta u \end{pmatrix} \begin{pmatrix} \frac{\partial u}{\partial x} \\ \frac{\partial v}{\partial x} \end{pmatrix} = \begin{pmatrix} f_1 \\ f_2 \end{pmatrix}, \tag{2.1}$$

where ϵ, η, α, and β are arbitrary constants and f_1 and f_2 are given continuous functions.

3 Discretization of problem

In this section, we apply the modal extended DG method to discretize the spatial dimension, which yields a system of ordinary differential equations. We then use the backward Euler method to solve the resulting system.

3.1 Modal extended DG method

We now address the modal extended DG method for the spatial discretization of problem (2.1). Let $\mathcal{E}_h = \{I_k\}_{k=1}^N$ be a partition of the domain Ω with the grid size $h_k = x_k - x_{k-1}$. The broken Sobolev space is defined by

$$H^s(\mathcal{E}_h) = \{v \in \mathcal{L}^2(\Omega) : \ v|_{I_k} \in H^s(I_k), \ k = 1, \ldots, N\}.$$

Thanks to the embedding theorem [22], s has to be chosen such that $s > \frac{3}{2}$. The space of discontinuous polynomials of degrees at most p is denoted by $\mathcal{D}_p(\mathcal{E}_h)$ and defined as $\mathcal{D}_p(\mathcal{E}_h) = \{v \in \mathcal{L}^2(\Omega) : \ v|_{I_k} \in \mathbb{P}_p(I_k), \ k = 1, \ldots, N\}$, where $\mathbb{P}_p(I_k)$ is the space of polynomials of degrees at most p on I_k , i.e., $\mathbb{P}_p(I_k) = span\{\psi_0^k, \ldots, \psi_p^k\}$, in which $\psi_i^k(x) = \begin{cases} \phi_i(\zeta^k), & x \in I_k, \\ 0, & x \notin I_k \end{cases}$, where the basis functions $\phi_i (i = 0, \ldots, p)$ are the Jacobi polynomials, which are modal basis functions, and the local variable $\zeta^k \in [-1, 1]$ are defined on I_k by the transformation function

$$\zeta^k = 2(x - x_{k-1})/(x_k - x_{k-1}) - 1. \tag{3.1}$$

The jump and average operators on $x_k = \overline{\partial I_k} \cap \overline{\partial I_{k+1}}$ are given by

$$[w(x_k)] = w|_{I_k}(x_k) - w|_{I_{k+1}}(x_k), \quad \{w(x_k)\} = 0.5(w|_{I_k}(x_k) + w|_{I_{k+1}}(x_k)),$$

and the jump and average at the x_0 and x_N are

$$[w(x_0)] = -w(x_0),\ [w(x_N)] = w(x_N),\ \{w(x_0)\} = w(x_0),\ \{w(x_N)\} = w(x_N).$$

Multiplying both sides of Equation (2.1) by $w \in \mathcal{D}_p(\mathcal{E}_h)$, integrating, and using integration by parts over the interval I_k, we get

$$\begin{aligned}&\int_{x_{k-1}}^{x_k} \begin{pmatrix} \frac{\partial u}{\partial t} w \\ \frac{\partial v}{\partial t} w \end{pmatrix} \mathrm{d}x + \epsilon \int_{x_{k-1}}^{x_k} \begin{pmatrix} \frac{\partial u}{\partial x} \frac{\partial w}{\partial x} \\ \frac{\partial v}{\partial x} \frac{\partial w}{\partial x} \end{pmatrix} \mathrm{d}x - \epsilon \begin{pmatrix} \frac{\partial u}{\partial x} w|_{x=x_k} - \frac{\partial u}{\partial x} w|_{x=x_{k-1}} \\ \frac{\partial v}{\partial x} w|_{x=x_k} - \frac{\partial v}{\partial x} w|_{x=x_{k-1}} \end{pmatrix} \\ &+ \int_{x_{k-1}}^{x_k} \begin{pmatrix} \frac{\eta}{2} \frac{\partial u^2}{\partial x_2} w + \alpha \frac{\partial (uv)}{\partial x} w \\ \frac{\xi}{2} \frac{\partial v^2}{\partial x} w + \beta \frac{\partial (uv)}{\partial x} w \end{pmatrix} \mathrm{d}x = \int_{x_{k-1}}^{x_k} \begin{pmatrix} f_1 w \\ f_2 w \end{pmatrix} \mathrm{d}x, \quad k = 1, \ldots, N.\end{aligned} \tag{3.2}$$

By summing all equations in (3.2), we obtain

$$\begin{aligned}&\sum_{k=1}^{N} \int_{x_{k-1}}^{x_k} \begin{pmatrix} \frac{\partial u}{\partial t} w \\ \frac{\partial v}{\partial t} w \end{pmatrix} \mathrm{d}x + \epsilon \sum_{k=1}^{N} \int_{x_{k-1}}^{x_k} \begin{pmatrix} \frac{\partial u}{\partial x} \frac{\partial w}{\partial x} \\ \frac{\partial v}{\partial x} \frac{\partial w}{\partial x} \end{pmatrix} \mathrm{d}x - \epsilon \sum_{k=0}^{N} \underbrace{\begin{pmatrix} [\frac{\partial u}{\partial x} w]|_{x=x_k} \\ [\frac{\partial v}{\partial x} w]|_{x=x_k} \end{pmatrix}}_{R_1} \\ &+ \sum_{k=1}^{N} \int_{x_{k-1}}^{x_k} \begin{pmatrix} \frac{\eta}{2} \frac{\partial u^2}{\partial x_2} w + \alpha \frac{\partial (uv)}{\partial x} w \\ \frac{\xi}{2} \frac{\partial v^2}{\partial x} w + \beta \frac{\partial (uv)}{\partial x} w \end{pmatrix} \mathrm{d}x = \sum_{k=1}^{N} \int_{x_{k-1}}^{x_k} \begin{pmatrix} f_1 w \\ f_2 w \end{pmatrix} \mathrm{d}x.\end{aligned} \tag{3.3}$$

If we apply the average and jump operators on the term R_1, then we get

$$\begin{pmatrix} [\frac{\partial u}{\partial x} w]|_{x=x_k} \\ [\frac{\partial v}{\partial x} w]|_{x=x_k} \end{pmatrix} = \underbrace{\begin{pmatrix} [\frac{\partial u}{\partial x}]\{w\}|_{x=x_k} \\ [\frac{\partial v}{\partial x}]\{w\}|_{x=x_k} \end{pmatrix}}_{R_2} + \underbrace{\begin{pmatrix} \{\frac{\partial u}{\partial x}\}[w]|_{x=x_k} \\ \{\frac{\partial v}{\partial x}\}[w]|_{x=x_k} \end{pmatrix}}_{R_3}.$$

There are two situations:

Case I. Since $\frac{\partial u}{\partial x}$ and $\frac{\partial v}{\partial x}$ are continuous functions, one can consider the term R_2 equals zero. To emphasize the continuity of u and v, we add penalty term to Equation (3.3)

$$\mathbf{J}_\sigma = \begin{pmatrix} J_{\sigma_u}(u, w) \\ J_{\sigma_v}(v, w) \end{pmatrix} = \begin{pmatrix} \sum_{k=0}^{N} \sigma_u [u][w]|_{x=x_k} \\ \sum_{k=0}^{N} \sigma_v [v][w]|_{x=x_k} \end{pmatrix}.$$

Therefore, we arrive at the following variational form of Equation (2.1):

$$\begin{aligned}&\sum_{k=1}^{N} \int_{x_{k-1}}^{x_k} \begin{pmatrix} \frac{\partial u}{\partial t} w \\ \frac{\partial v}{\partial t} w \end{pmatrix} \mathrm{d}x + \epsilon \sum_{k=1}^{N} \int_{x_{k-1}}^{x_k} \begin{pmatrix} \frac{\partial u}{\partial x} \frac{\partial w}{\partial x} \\ \frac{\partial v}{\partial x} \frac{\partial w}{\partial x} \end{pmatrix} \mathrm{d}x - \epsilon \sum_{k=0}^{N} \begin{pmatrix} \{\frac{\partial u}{\partial x}\}[w]|_{x=x_k} \\ \{\frac{\partial v}{\partial x}\}[w]|_{x=x_k} \end{pmatrix} \\ &\quad + \sum_{k=1}^{N} \int_{x_{k-1}}^{x_k} \begin{pmatrix} \frac{\eta}{2} \frac{\partial u^2}{\partial x_2} w + \alpha \frac{\partial (uv)}{\partial x} w \\ \frac{\xi}{2} \frac{\partial v^2}{\partial x} w + \beta \frac{\partial (uv)}{\partial x} w \end{pmatrix} \mathrm{d}x + \begin{pmatrix} \sum_{k=0}^{N} \sigma_u [u][w]|_{x=x_k} \\ \sum_{k=0}^{N} \sigma_v [v][w]|_{x=x_k} \end{pmatrix} \\ &\quad = \sum_{k=1}^{N} \int_{x_{k-1}}^{x_k} \begin{pmatrix} f_1 w \\ f_2 w \end{pmatrix} \mathrm{d}x.\end{aligned}$$

Case II. To insist on the continuity of $\frac{\partial u}{\partial x}$ and $\frac{\partial v}{\partial x}$, in addition to $\mathbf{J}_\sigma$, we add

$$\mathbf{J}_{\sigma_x} = \begin{pmatrix} J_{\sigma_{u_x}}(u,w) \\ J_{\sigma_{v_x}}(v,w) \end{pmatrix} = \begin{pmatrix} \sum_{k=0}^{N} \sigma_{u_x} [\frac{\partial u}{\partial x}][\frac{\partial w}{\partial x}]|_{x=x_k} \\ \sum_{k=0}^{N} \sigma_{v_x} [\frac{\partial v}{\partial x}][\frac{\partial w}{\partial x}]|_{x=x_k} \end{pmatrix}$$

to Equation (3.3). In fact, in this case the term R_2 is not equal to zero.

Hereafter, we derive the discrete form of Case II. In a possibly similar way, one may get the discrete form of Case I. Based on the DG method, the approximate global solutions are defined as follows:

$$\hat{u} = \sum_{k=1}^{N} \sum_{i=0}^{p} a_i^k(t)\psi_i^k(x) = \sum_{k=1}^{N} \Psi^k(x)(\mathbf{a}^k(t))^T = \Psi(x)(\mathbf{a}(t))^T, \tag{3.4}$$

$$\hat{v} = \sum_{k=1}^{N} \sum_{i=0}^{p} b_i^k(t)\psi_i^k(x) = \sum_{k=1}^{N} \Psi^k(x)(\mathbf{b}^k(t))^T = \Psi(x)(\mathbf{b}(t))^T, \tag{3.5}$$

where $\mathbf{a}(t) = [\mathbf{a}^1(t), \ldots, \mathbf{a}^N(t)]$, $\mathbf{b}(t) = [\mathbf{b}^1(t), \ldots, \mathbf{b}^N(t)]$ and $\Psi(x) = [\Psi^1(x), \ldots, \Psi^N(x)]$, in which $\mathbf{a}^k(t) = [a_0^k(t), \ldots, a_p^k(t)]$ and $\Psi^k(x) = [\psi_0^k(x), \ldots, \psi_p^k(x)]$. Choosing the test function, w, from $\Psi(x)$ and substituting the global approximate solutions (3.4) and (3.5) in the variational form of Equation (2.1), we get the following system of ODEs for the $\mathbf{a}(t)$ and $\mathbf{b}(t)$ for $j = 0, 1, \ldots, p$:

$$\begin{aligned}
&\sum_{k=1}^{N} \begin{pmatrix} \sum_{i=0}^{p} \frac{\partial a_i^k(t)}{\partial t} \int_{x_{k-1}}^{x_k} \psi_i^k(x)\psi_j^k(x)\,\mathrm{d}x \\ \sum_{i=0}^{p} \frac{\partial b_i^k(t)}{\partial t} \int_{x_{k-1}}^{x_k} \psi_i^k(x)\psi_j^k(x)\,\mathrm{d}x \end{pmatrix} \\
&\quad + \epsilon \sum_{k=1}^{N} \begin{pmatrix} \sum_{i=0}^{p} a_i^k(t) \int_{x_{k-1}}^{x_k} \frac{\partial \psi_i^k(x)}{\partial x} \frac{\partial \psi_j^k(x)}{\partial x}\,\mathrm{d}x \\ \sum_{i=0}^{p} b_i^k(t) \int_{x_{k-1}}^{x_k} \frac{\partial \psi_i^k(x)}{\partial x} \frac{\partial \psi_j^k(x)}{\partial x}\,\mathrm{d}x \end{pmatrix} \\
&- \epsilon \sum_{k=1}^{N} \begin{pmatrix} \sum_{i=0}^{p} a_i^k(t) \Big(\frac{\partial \psi_i^k(x)}{\partial x}|_{x=x_k} \psi_j^k(x_k) - \frac{\partial \psi_i^k(x)}{\partial x}|_{x=x_{k-1}} \psi_j^k(x_{k-1}) \Big) \\ \sum_{i=0}^{p} b_i^k(t) \Big(\frac{\partial \psi_i^k(x)}{\partial x}|_{x=x_k} \psi_j^k(x_k) - \frac{\partial \psi_i^k(x)}{\partial x}|_{x=x_{k-1}} \psi_j^k(x_{k-1}) \Big) \end{pmatrix} \\
&+ \sum_{k=1}^{N} \begin{pmatrix} \eta \int_{x_{k-1}}^{x_k} (\sum_{i=0}^{p} a_i^k(t)\psi_i^k(x))(\sum_{i=0}^{p} a_i^k(t) \frac{\partial \psi_i^k(x)}{\partial x}) \psi_j^k(x)\,\mathrm{d}x \\ \xi \int_{x_{k-1}}^{x_k} (\sum_{i=0}^{p} b_i^k(t)\psi_i^k(x))(\sum_{i=0}^{p} b_i^k(t) \frac{\partial \psi_i^k(x)}{\partial x}) \psi_j^k(x)\,\mathrm{d}x \end{pmatrix} \\
&+ \sum_{k=1}^{N} \begin{pmatrix} \alpha \int_{x_{k-1}}^{x_k} (\sum_{i=0}^{p} a_i^k(t) \frac{\partial \psi_i^k(x)}{\partial x})(\sum_{i=0}^{p} b_i^k(t)\psi_i^k(x)) \psi_j^k(x)\,\mathrm{d}x \\ \beta \int_{x_{k-1}}^{x_k} (\sum_{i=0}^{p} b_i^k(t) \frac{\partial \psi_i^k(x)}{\partial x})(\sum_{i=0}^{p} a_i^k(t)\psi_i^k(x)) \psi_j^k(x)\,\mathrm{d}x \end{pmatrix} \\
&+ \sum_{k=1}^{N} \begin{pmatrix} \alpha \int_{x_{k-1}}^{x_k} (\sum_{i=0}^{p} a_i^k(t)\psi_i^k(x))(\sum_{i=0}^{p} b_i^k(t) \frac{\partial \psi_i^k(x)}{\partial x}) \psi_j^k(x)\,\mathrm{d}x \\ \beta \int_{x_{k-1}}^{x_k} (\sum_{i=0}^{p} b_i^k(t)\psi_i^k(x))(\sum_{i=0}^{p} a_i^k(t) \frac{\partial \psi_i^k(x)}{\partial x}) \psi_j^k(x)\,\mathrm{d}x \end{pmatrix} \\
&+ \begin{pmatrix} \sum_{k=1}^{N} \sigma_{u_x} \sum_{i=0}^{p} a_i^k(t) \Big((\frac{\partial \psi_i^k(x)}{\partial x} \frac{\partial \psi_j^k(x)}{\partial x})|_{x=x_k} + (\frac{\partial \psi_i^k(x)}{\partial x} \frac{\partial \psi_j^k(x)}{\partial x})|_{x=x_{k-1}} \Big) \\ \sum_{k=1}^{N} \sigma_{v_x} \sum_{i=0}^{p} b_i^k(t) \Big((\frac{\partial \psi_i^k(x)}{\partial x} \frac{\partial \psi_j^k(x)}{\partial x})|_{x=x_k} + (\frac{\partial \psi_i^k(x)}{\partial x} \frac{\partial \psi_j^k(x)}{\partial x})|_{x=x_{k-1}} \Big) \end{pmatrix}
\end{aligned}$$

$$
\begin{aligned}
&- \begin{pmatrix} \sum_{k=1}^{N} \sigma_{u_x} \sum_{i=0}^{p} a_i^{k+1}(t)(\frac{\partial \psi_i^{k+1}(x)}{\partial x} \frac{\partial \psi_j^{k}(x)}{\partial x})|_{x=x_k} \\ \sum_{k=1}^{N} \sigma_{v_x} \sum_{i=0}^{p} b_i^{k+1}(t)(\frac{\partial \psi_i^{k+1}(x)}{\partial x} \frac{\partial \psi_j^{k}(x)}{\partial x})|_{x=x_k} \end{pmatrix} \\
&- \begin{pmatrix} \sum_{k=1}^{N} \sigma_{u_x} \sum_{i=0}^{p} a_i^{k-1}(t)(\frac{\partial \psi_i^{k-1}(x)}{\partial x} \frac{\partial \psi_j^{k}(x)}{\partial x})|_{x=x_{k-1}} \\ \sum_{k=1}^{N} \sigma_{v_x} \sum_{i=0}^{p} b_i^{k-1}(t)(\frac{\partial \psi_i^{k-1}(x)}{\partial x} \frac{\partial \psi_j^{k}(x)}{\partial x})|_{x=x_{k-1}} \end{pmatrix} \\
&+ \begin{pmatrix} \sum_{k=1}^{N} \sigma_{u} \sum_{i=0}^{p} a_i^{k}(t)\Big(\psi_i^k(x_k)\psi_j^k(x_k) + \psi_i^k(x_{k-1})\psi_j^k(x_{k-1})\Big) \\ \sum_{k=1}^{N} \sigma_{v} \sum_{i=0}^{p} b_i^{k}(t)\Big(\psi_i^k(x_k)\psi_j^k(x_k) + \psi_i^k(x_{k-1})\psi_j^k(x_{k-1})\Big) \end{pmatrix} \\
&- \begin{pmatrix} \sum_{k=1}^{N} \sigma_{u} \sum_{i=0}^{p} a_i^{k+1}(t)\psi_i^{k+1}(x_k)\psi_j^k(x_k) \\ \sum_{k=1}^{N} \sigma_{v} \sum_{i=0}^{p} b_i^{k+1}(t)\psi_i^{k+1}(x_k)\psi_j^k(x_k) \end{pmatrix} \\
&- \begin{pmatrix} \sum_{k=1}^{N} \sigma_{u} \sum_{i=0}^{p} a_i^{k-1}(t)\psi_i^{k-1}(x_{k-1})\psi_j^k(x_{k-1}) \\ \sum_{k=1}^{N} \sigma_{v} \sum_{i=0}^{p} b_i^{k-1}(t)\psi_i^{k-1}(x_{k-1})\psi_j^k(x_{k-1}) \end{pmatrix} = \sum_{k=1}^{N} \begin{pmatrix} \int_{x_{k-1}}^{x_k} f_1 \psi_j^k(x)\ \mathrm{d}x \\ \int_{x_{k-1}}^{x_k} f_2 \psi_j^k(x)\ \mathrm{d}x \end{pmatrix}.
\end{aligned} \tag{3.6}
$$

3.2 Time splitting method

We employ the backward Euler method to approximate the time derivative in the system of equations (3.6). To do this, let the time interval be $[0, T_f]$, $\Delta t > 0$ be the time step, $t^n = n\Delta t$, $u^n = u(x, t^n)$, $v^n = v(x, t^n)$, and $f_i^n = f_i(x, t^n)$, $i = 1, 2$. Therefore, we have

$$
\begin{aligned}
&\sum_{k=1}^{N} \sum_{i=0}^{p} \frac{a_i^k(t^{n+1}) - a_i^k(t^n)}{\Delta t} \int_{x_{k-1}}^{x_k} \psi_i^k(x)\psi_j^k(x)\ \mathrm{d}x \\
&+ \epsilon \sum_{k=1}^{N} \sum_{i=0}^{p} a_i^k(t^{n+1}) \int_{x_{k-1}}^{x_k} \frac{\partial \psi_i^k(x)}{\partial x} \frac{\partial \psi_j^k(x)}{\partial x}\ \mathrm{d}x \\
&- \epsilon \sum_{k=1}^{N} \sum_{i=0}^{p} a_i^k(t^{n+1}) \Big(\frac{\partial \psi_i^k(x)}{\partial x}|_{x=x_k} \psi_j^k(x_k) - \frac{\partial \psi_i^k(x)}{\partial x}|_{x=x_{k-1}} \psi_j^k(x_{k-1}) \Big) \\
&+ \sum_{k=1}^{N} \eta \int_{x_{k-1}}^{x_k} (\sum_{i=0}^{p} a_i^k(t^{n+1})\psi_i^k(x))(\sum_{i=0}^{p} a_i^k(t^{n+1}) \frac{\partial \psi_i^k(x)}{\partial x})\psi_j^k(x)\ \mathrm{d}x \\
&+ \sum_{k=1}^{N} \alpha \int_{x_{k-1}}^{x_k} (\sum_{i=0}^{p} a_i^k(t^{n+1}) \frac{\partial \psi_i^k(x)}{\partial x})(\sum_{i=0}^{p} b_i^k(t^n)\psi_i^k(x))\psi_j^k(x)\ \mathrm{d}x \\
&+ \sum_{k=1}^{N} \alpha \int_{x_{k-1}}^{x_k} (\sum_{i=0}^{p} a_i^k(t^{n+1})\psi_i^k(x))(\sum_{i=0}^{p} b_i^k(t^n) \frac{\partial \psi_i^k(x)}{\partial x})\psi_j^k(x)\ \mathrm{d}x \\
&+ \sum_{k=1}^{N} \sigma_u \sum_{i=0}^{p} a_i^k(t^{n+1}) \Big(\psi_i^k(x_k)\psi_j^k(x_k) + \psi_i^k(x_{k-1})\psi_j^k(x_{k-1}) \Big) - \sum_{k=1}^{N} \sigma_u \sum_{i=0}^{p} \\
&\times a_i^{k+1}(t^{n+1})\psi_i^{k+1}(x_k)\psi_j^k(x_k) - \sum_{k=1}^{N} \sigma_u \sum_{i=0}^{p} a_i^{k-1}(t^{n+1})\psi_i^{k-1}(x_{k-1})\psi_j^k(x_{k-1})
\end{aligned}
$$

$$
\begin{aligned}
&+\sum_{k=1}^{N}\sigma_{u_x}\sum_{i=0}^{p}a_i^k(t^{n+1})\Big((\frac{\partial\psi_i^k(x)}{\partial x}\frac{\partial\psi_j^k(x)}{\partial x})|_{x=x_k}+(\frac{\partial\psi_i^k(x)}{\partial x}\frac{\partial\psi_j^k(x)}{\partial x})|_{x=x_{k-1}}\Big)\\
&-\sum_{k=1}^{N}\sigma_{u_x}\sum_{i=0}^{p}a_i^{k+1}(t^{n+1})(\frac{\partial\psi_i^{k+1}(x)}{\partial x}\frac{\partial\psi_j^k(x)}{\partial x})|_{x=x_k}\\
&-\sum_{k=1}^{N}\sigma_{u_x}\sum_{i=0}^{p}a_i^{k-1}(t^{n+1})(\frac{\partial\psi_i^{k-1}(x)}{\partial x}\frac{\partial\psi_j^k(x)}{\partial x})|_{x=x_{k-1}}\\
&-\sum_{k=1}^{N}\int_{x_{k-1}}^{x_k}f_1^{n+1}\psi_j^k(x)\,\mathrm{d}x=0,\quad j=0,1,\ldots,p. \qquad (3.7)
\end{aligned}
$$

The above resulting fully discrete scheme yields a non-linear system of $N(p+1)$ equations for $\mathbf{a}(t^{n+1})$ in each time step, t^n. We use the Newton method to solve (3.7) for $\mathbf{a}(t^{n+1})$. The Newton method is an iterative method that, in each iteration, leads to the following linear system of equations:

$$
\mathbf{J}_{\mathbf{F_a}}(\mathbf{a}(t^{m+1})-\mathbf{a}(t^m))=-\mathbf{F}(\mathbf{a}(t^m)),\quad m=0,1,\ldots, \qquad (3.8)
$$

where the vector $\mathbf{F}$ is the right-hand side of Equation (3.7) and $\mathbf{J}_{\mathbf{F_a}}$ is the Jacobian matrix of $\mathbf{F}$, which is a tridiagonal block matrix, with the following structure:

$$
M_u=\begin{pmatrix}
A_u^1 & B^1 & & & & \\
C^2 & A_u^2 & B^2 & & & \\
 & \cdots & \cdots & \cdots & & \\
 & & & C^{N-1} & A_u^{N-1} & B^{N-1}\\
 & & & & C^N & A_u^N
\end{pmatrix},
$$

where $(i,j=0,1,\ldots,p.)$

$$
\begin{aligned}
(A_u^k)_{ij}&=\frac{1}{\Delta t}\int_{x_{k-1}}^{x_k}\psi_i^k(x)\psi_j^k(x)\,\mathrm{d}x+\epsilon\int_{x_{k-1}}^{x_k}\frac{\partial\psi_i^k(x)}{\partial x}\frac{\partial\psi_j^k(x)}{\partial x}\,\mathrm{d}x\\
&-\epsilon\Big(\frac{\partial\psi_i^k(x)}{\partial x}|_{x=x_k}\psi_j^k(x_k)-\frac{\partial\psi_i^k(x)}{\partial x}|_{x=x_{k-1}}\psi_j^k(x_{k-1})\Big)\\
&+\eta\int_{x_{k-1}}^{x_k}\psi_i^k(x)\underbrace{(\sum_{i=0}^{p}a_i^k(t^m)\frac{\partial\psi_i^k(x)}{\partial x})}_{\frac{\partial u^m}{\partial x}}\psi_j^k(x)\,\mathrm{d}x\\
&+\eta\int_{x_{k-1}}^{x_k}\underbrace{(\sum_{i=0}^{p}a_i^k(t^{m+1})\psi_i^k(x))}_{u^m}\frac{\partial\psi_i^k(x)}{\partial x}\psi_j^k(x)\,\mathrm{d}x\\
&+\alpha\int_{x_{k-1}}^{x_k}\frac{\partial\psi_i^k(x)}{\partial x}\underbrace{(\sum_{i=0}^{p}b_i^k(t^m)\psi_i^k(x))}_{v^m}\psi_j^k(x)\,\mathrm{d}x
\end{aligned}
$$

$$
\begin{aligned}
&+\alpha\int_{x_{k-1}}^{x_k}\psi_i^k(x)\underbrace{(\sum_{i=0}^{p}b_i^k(t^m)\frac{\partial\psi_i^k(x)}{\partial x})}_{\frac{\partial v^m}{\partial x}}\psi_j^k(x)\,\mathrm{d}x\\
&+\sigma_u\Big(\psi_i^k(x_k)\psi_j^k(x_k)+\psi_i^k(x_{k-1})\psi_j^k(x_{k-1})\Big)\\
&+\sigma_{u_x}\Big((\frac{\partial\psi_i^k(x)}{\partial x}\frac{\partial\psi_j^k(x)}{\partial x})|_{x=x_k}+(\frac{\partial\psi_i^k(x)}{\partial x}\frac{\partial\psi_j^k(x)}{\partial x})|_{x=x_{k-1}}\Big),\\
(B^k)_{ij}=&-\sigma_{u_x}(\frac{\partial\psi_i^{k+1}(x)}{\partial x}\frac{\partial\psi_j^k(x)}{\partial x})|_{x=x_k}-\sigma_u(\psi_i^{k+1}(x_k)\psi_j^k(x_k)),\\
(C^k)_{ij}=&-\sigma_{u_x}(\frac{\partial\psi_i^{k-1}(x)}{\partial x}\frac{\partial\psi_j^k(x)}{\partial x})|_{x=x_{k-1}}-\sigma_u(\psi_i^{k-1}(x_{k-1})\psi_j^k(x_{k-1})).
\end{aligned}
$$

The solving process of Equation (3.8) is repeated until the desired accuracy, $\| \mathbf{a}(t^{m+1})-\mathbf{a}(t^m)\| \le \varepsilon$, where ε is the certain criterion error is reached. In this way, we obtain $\mathbf{a}(t^{n+1})$. Substituting $\mathbf{a}(t^{n+1})$ into Equation (3.4), we get $\hat{u}^{n+1}$. Using the same procedure for the second Equation of (3.6), one can find the value of $\mathbf{b}(t^{n+1})$ and get $\hat{v}^{n+1}$ from Equation (3.5).

4 Stability analysis

In this section, we investigate the stability analysis of the IEDG scheme to find the appropriate ranges for penalty terms and the time step. We obtain a suitable range of each parameter in Case II. Applying the backward Euler method to Equation (3.6), we have

$$
\begin{aligned}
&\sum_{k=1}^{N}\int_{x_{k-1}}^{x_k}\begin{pmatrix}\frac{u^{n+1}-u^n}{\Delta t}w\\ \frac{v^{n+1}-v^n}{\Delta t}w\end{pmatrix}\mathrm{d}x+\epsilon\sum_{k=1}^{N}\int_{x_{k-1}}^{x_k}\begin{pmatrix}\frac{\partial u^{n+1}}{\partial x}\frac{\partial w}{\partial x}\\ \frac{\partial v^{n+1}}{\partial x}\frac{\partial w}{\partial x}\end{pmatrix}\mathrm{d}x\\
&-\epsilon\sum_{k=0}^{N}\begin{pmatrix}\{\frac{\partial u^{n+1}}{\partial x}\}[w]|_{x=x_k}\\ \{\frac{\partial v^{n+1}}{\partial x}\}[w]|_{x=x_k}\end{pmatrix}-\epsilon\sum_{k=0}^{N}\begin{pmatrix}[\frac{\partial u^{n+1}}{\partial x}]\{w\}|_{x=x_k}\\ [\frac{\partial v^{n+1}}{\partial x}]\{w\}|_{x=x_k}\end{pmatrix}\\
&+\sum_{k=0}^{N}\begin{pmatrix}\sigma_u[u^{n+1}][w]|_{x=x_k}\\ \sigma_v[v^{n+1}][w]|_{x=x_k}\end{pmatrix}+\sum_{k=0}^{N}\begin{pmatrix}\sigma_{u_x}[\frac{\partial u^{n+1}}{\partial x}][\frac{\partial w}{\partial x}]|_{x=x_k}\\ \sigma_{v_x}[\frac{\partial v^{n+1}}{\partial x}][\frac{\partial w}{\partial x}]|_{x=x_k}\end{pmatrix}\\
&+\sum_{k=1}^{N}\int_{x_{k-1}}^{x_k}\begin{pmatrix}\frac{\eta}{2}\frac{\partial(u^{n+1})^2}{\partial x}w+\alpha\frac{\partial(u^{n+1}v^{n+1})}{\partial x}w\\ \frac{\xi}{2}\frac{\partial(v^{n+1})^2}{\partial x}w+\beta\frac{\partial(u^{n+1}v^{n+1})}{\partial x}w\end{pmatrix}\mathrm{d}x=\sum_{k=1}^{N}\int_{x_{k-1}}^{x_k}\begin{pmatrix}f_1^{n+1}w\\ f_2^{n+1}w\end{pmatrix}\mathrm{d}x. \quad (4.1)
\end{aligned}
$$

Decoupling the above system of equations and inserting $\hat{u}$ instead of u, we find

$$
\begin{aligned}
&\sum_{k=1}^{N}\int_{x_{k-1}}^{x_k}\frac{\hat{u}^{n+1}-\hat{v}^n}{\Delta t}w\,\mathrm{d}x+\epsilon\sum_{k=1}^{N}\int_{x_{k-1}}^{x_k}\frac{\partial\hat{u}^{n+1}}{\partial x}\frac{\partial w}{\partial x}\,\mathrm{d}x-\epsilon\sum_{k=0}^{N}\{\frac{\partial\hat{u}^{n+1}}{\partial x}\}[w]|_{x=x_k}\\
&-\epsilon\sum_{k=0}^{N}[\frac{\partial\hat{u}^{n+1}}{\partial x}]\{w\}|_{x=x_k}+\sum_{k=1}^{N}\int_{x_{k-1}}^{x_k}(\frac{\eta}{2}\frac{\partial(\hat{u}^{n+1})^2}{\partial x}w+\alpha\frac{\partial(\hat{u}^{n+1}\hat{v}^n)}{\partial x})w\,\mathrm{d}x
\end{aligned}
$$

$$+\sum_{k=0}^{N}\sigma_u[\hat{u}^{n+1}][w]|_{x=x_k}+\sum_{k=0}^{N}\sigma_{u_x}[\frac{\partial\hat{u}^{n+1}}{\partial x}][\frac{\partial w}{\partial x}]|_{x=x_k}=\sum_{k=1}^{N}\int_{x_{k-1}}^{x_k}f_1^{n+1}w\ \mathrm{d}x. \quad (4.2)$$

The structure of the second equation of (4.1), and therefore its stability analysis, is similar to Equation (4.2). Thus, we only provide the stability analysis of (4.2). In the following theorem, we obtain the constants of the inverse trace inequality based on the idea in [12]:

Theorem 1. *Let, for $k=1,\dots,N$, $I_k=[x_{k-1},x_k]$, and $\mathbb{P}_p(I_k)$ be the space of polynomials spanned by the Legendre polynomials of order p as the basis functions. Then for all $z\in\mathbb{P}_p(I_k)$, the following results hold:*

$$|z(x_k)|\le\frac{p+1}{\sqrt{x_k-x_{k-1}}}\|z\|_{\mathcal{L}^2(I_k)}, \quad (4.3)$$

$$\left|\frac{dz(x)}{dx}\Big|_{x=x_k}\right|\le\sqrt{(p^2+1)/(x_k-x_{k-1})}\left\|\frac{dz}{dx}\right\|_{\mathcal{L}^2(I_k)}. \quad (4.4)$$

Proof. We first derive the value of constants of inequalities on the reference domain $[-1,1]$ with coordinate ζ. To prove (4.4), we consider the value of $\frac{d_z(\zeta)}{d\zeta}$ at one endpoint of the interval, e.g., -1. Regarding Equation (3.4), we have

$$\left(\frac{\mathrm{d}z(\zeta)}{\mathrm{d}\zeta}\Big|_{\zeta=-1}\right)^2=\mathbf{a}(t)\underbrace{\left(\frac{\mathrm{d}\Psi(\zeta)}{\mathrm{d}\zeta}\Big|_{\zeta=-1}\right)^T\frac{\mathrm{d}\Psi(\zeta)}{\mathrm{d}\zeta}\Big|_{\zeta=-1}}_{A_1}(\mathbf{a}(t))^T,$$

where A_1 is an $N(p+1)$ by $N(p+1)$ symmetric matrix. Also, we have

$$\int_{-1}^{1}\left(\frac{\mathrm{d}z(\zeta)}{\mathrm{d}\zeta}\right)^2\mathrm{d}\zeta=\mathbf{a}(t)\underbrace{\int_{-1}^{1}\left(\frac{\mathrm{d}\Psi(\zeta)}{\mathrm{d}\zeta}\right)^T\frac{\mathrm{d}\Psi(\zeta)}{\mathrm{d}\zeta}\,\mathrm{d}\zeta}_{A_0}(\mathbf{a}(t))^T,$$

where A_0 is an $N(p+1)$ by $N(p+1)$ symmetric matrix. We want to find $C_1(p)$ that satisfies

$$\big(\frac{\mathrm{d}z(\zeta)}{\mathrm{d}\zeta}|_{\zeta=-1}\big)^2\le C_1(p)\int_{-1}^{1}\big(\frac{\mathrm{d}z(\zeta)}{\mathrm{d}\zeta}\big)^2\,\mathrm{d}\zeta,$$

i.e., $\mathbf{a}(t)\big(C_1(p)A_0-A_1\big)(\mathbf{a}(t))^T\ge 0$. Thus it is sufficient to choose $C_1(p)$ such that the matrix $(C_1(p)A_0-A_1)$ be positive semidefinite. By some computational efforts, one can obtain the recurrence relation depending on the degree of the polynomials as $C_1(p)-C_1(p-2)=2p-2,\ C_1(1)=1,\ C_1(2)=\frac{5}{2},\ p\ge 3$, which its solution is $C_1(p)=\frac{P^2+1}{2}$. Using the transformation function (3.1), we have $|\frac{dz(x)}{\mathrm{d}x}|_{x=x_k}|\le\sqrt{\frac{P^2+1}{x_k-x_{k-1}}}\|\frac{dz}{\mathrm{d}x}\|_{\mathcal{L}^2(I_k)}$, which proves (4.4). To prove (4.3), starting from Equation (3.4), we wish to find $C_0(p)$ satisfies $z(-1)^2\le C_0(p)\int_{-1}^{1}z(\zeta)^2\,\mathrm{d}\zeta$. Now, similarly, one can get the recurrence relation $C_0(p)-C_0(p-2)=2p,\ C_0(1)=2,\ C_0(2)=9/2,\ p\ge 3$. The solution of the above relation is $C_0(p)=(p+1)^2/2$. It is easy to obtain (4.3) by transferring the reference domain to I_k using (3.1). □

In the next theorem, stability conditions for Equation (4.2) are addressed and proved.

Theorem 2. *Assume that* $\Delta t < \min(1/C_1, 1/C_2)$, *where for Case I*

$$\begin{aligned} C_1 =& \frac{2|\eta|}{3h_e}\Big(\max_{k=0,\dots,N}\hat{u}^0(x_k)\Big)(p+1)^2 + \frac{|\alpha|}{h_e}\Big(\max_{k=0,\dots,N}\hat{v}^0(x_k)\Big)(p+1)^2 \\ & - |\alpha|\max_{x\in\Omega}\frac{\partial\hat{v}^0}{\partial x} + \theta_1, \\ C_2 =& \frac{2|\xi|}{3h_e}\Big(\max_{k=0,\dots,N}\hat{v}^0(x_k)\Big)(p+1)^2 + \frac{|\beta|}{h_e}\Big(\max_{k=0,\dots,N}\hat{u}^0(x_k)\Big)(p+1)^2 \\ & - |\beta|\max_{x\in\Omega}\frac{\partial\hat{u}^0}{\partial x} + \theta_2, \end{aligned}$$

and for Case II

$$\begin{aligned} C_1 =& \frac{\epsilon}{h_e}(p+1)^2 + \frac{2|\eta|}{3h_e}\Big(\max_{k=0,\dots,N}\hat{u}^0(x_k)\Big)(p+1)^2 \\ & + \frac{|\alpha|}{h_e}\Big(\max_{k=0,\dots,N}\hat{v}^0(x_k)\Big)(p+1)^2 - |\alpha|\max_{x\in\Omega}\frac{\partial\hat{v}^0}{\partial x} + \theta_1, \\ C_2 =& \frac{\epsilon}{h_e}(p+1)^2 + \frac{2|\xi|}{3h_e}\Big(\max_{k=0,\dots,N}\hat{v}^0(x_k)\Big)(p+1)^2 \\ & + \frac{|\beta|}{h_e}\Big(\max_{k=0,\dots,N}\hat{u}^0(x_k)\Big)(p+1)^2 - |\beta|\max_{x\in\Omega}\frac{\partial\hat{u}^0}{\partial x} + \theta_2, \end{aligned}$$

in which $h_e = \min_{k=1,\dots,N}(x_k - x_{k-1})$,

$$\theta_1 = \begin{cases} 1, & f_1 \neq 0, \\ 0, & f_1 = 0, \end{cases}, \quad \theta_2 = \begin{cases} 1, & f_2 \neq 0, \\ 0, & f_2 = 0. \end{cases}$$

Then, for all $m \geq 0$,

$$\sum_{k=1}^{N}\|\hat{u}^m\|^2_{\mathcal{L}^2(I_k)} \leq e^{C_1(m+1)\Delta t}\Big(\sum_{k=1}^{N}\|\hat{u}^0\|^2_{\mathcal{L}^2(I_k)} + \theta_1\Delta t\sum_{n=1}^{m}\sum_{k=1}^{N}\|f_1^n\|^2_{\mathcal{L}^2(\Omega)}\Big), \tag{4.5}$$

$$\sum_{k=1}^{N}\|\hat{v}^m\|^2_{\mathcal{L}^2(I_k)} \leq e^{C_2(m+1)\Delta t}\Big(\sum_{k=1}^{N}\|\hat{v}^0\|^2_{\mathcal{L}^2(I_k)} + \theta_2\Delta t\sum_{n=1}^{m}\sum_{k=1}^{N}\|f_2^n\|^2_{\mathcal{L}^2(\Omega)}\Big). \tag{4.6}$$

Proof. We only prove inequality (4.5). The proof of inequality (4.6) is similar. Taking $w = \hat{u}^{n+1}$ and using $(a-b)a \geq \frac{1}{2}(a^2 - b^2)$, (4.2) can be rewritten

$$\sum_{k=1}^{N}\frac{1}{2\Delta t}(\|\hat{u}^{n+1}\|^2_{\mathcal{L}^2(I_k)} - \|\hat{u}^n\|^2_{\mathcal{L}^2(I_k)}) + \epsilon\sum_{k=1}^{N}\Big\|\frac{\partial\hat{u}^{n+1}}{\partial x}\Big\|^2_{\mathcal{L}^2(I_k)}$$

$$
\begin{aligned}
&\underbrace{-\epsilon\sum_{k=0}^{N}(\{\frac{\partial\hat{u}^{n+1}}{\partial x}\}[\hat{u}^{n+1}])_{x=x_k}}_{R_5}+\sum_{k=0}^{N}\sigma_u[\hat{u}^{n+1}]^2_{x=x_k}\underbrace{-\epsilon\sum_{k=0}^{N}([\frac{\partial\hat{u}^{n+1}}{\partial x}]\{\hat{u}^{n+1}\})_{x=x_k}}_{R_6}\\
&+\sum_{k=0}^{N}\sigma_{u_x}[\frac{\partial\hat{u}^{n+1}}{\partial x}]^2_{x=x_k}+\sum_{k=0}^{N}\frac{\eta}{3}[(\hat{u}^{n+1})^3]_{x=x_k}+\sum_{k=0}^{N}\frac{\alpha}{2}[(\hat{u}^{n+1})^2\hat{v}^n]_{x=x_k}\\
&+\sum_{k=1}^{N}\int_{x_{k-1}}^{x_k}\frac{\alpha}{2}(\hat{u}^{n+1})^2\frac{\partial\hat{u}^n}{\partial x}\,\mathrm{d}x-\underbrace{\sum_{k=1}^{N}\theta_1\int_{x_{k-1}}^{x_k}f_1^{n+1}\hat{u}^{n+1}\,\mathrm{d}x}_{R_7}\le 0. \qquad (4.7)
\end{aligned}
$$

Now, we are going to find upper bounds for terms R_5, R_6, and R_7 by using Young's inequality as follows:

$$
\begin{aligned}
&\{\frac{\partial\hat{u}^{n+1}}{\partial x}\}[\hat{u}^{n+1}]\le\frac{\gamma_1}{2}(\{\frac{\partial\hat{u}^{n+1}}{\partial x}\})^2+\frac{1}{2\gamma_1}([\hat{u}^{n+1}])^2,\\
&[\frac{\partial\hat{u}^{n+1}}{\partial x}]\{\hat{u}^{n+1}\}\le\frac{1}{2}([\frac{\partial\hat{u}^{n+1}}{\partial x}])^2+\frac{1}{2}(\{\hat{u}^{n+1}\})^2, \qquad (4.8)\\
&\theta_1\int_{x_{k-1}}^{x_k}f_1^{n+1}\hat{u}^{n+1}\,\mathrm{d}x\le\frac{\theta_1}{2}\|f_1^{n+1}\|^2_{\mathcal{L}^2(I_k)}+\frac{\theta_1}{2}\|\hat{u}^{n+1}\|^2_{\mathcal{L}^2(I_k)}.
\end{aligned}
$$

Substituting (4.8) into (4.7), we obtain

$$
\begin{aligned}
&\sum_{k=1}^{N}\frac{1}{2\Delta t}(\|\hat{u}^{n+1}\|^2_{\mathcal{L}^2(I_k)}-\|\hat{u}^{n}\|^2_{\mathcal{L}^2(I_k)})+\epsilon\sum_{k=1}^{N}\Big\|\frac{\partial\hat{u}^{n+1}}{\partial x}\Big\|^2_{\mathcal{L}^2(I_k)}\\
&-\epsilon\sum_{k=0}^{N}\underbrace{\frac{\gamma_1}{2}(\{\frac{\partial\hat{u}^{n+1}}{\partial x}\}|_{x=x_k})^2}_{R_8}+\sum_{k=0}^{N}(\sigma_u-\frac{\epsilon}{2\gamma_1})[\hat{u}^{n+1}]^2_{x=x_k}+\sum_{k=0}^{N}\frac{\eta}{3}[(\hat{u}^{n+1})^3]_{x=x_k}\\
&-\epsilon\sum_{k=0}^{N}\frac{1}{2}(\{\hat{u}^{n+1}\}|_{x=x_k})^2+\sum_{k=0}^{N}(\sigma_{u_x}-\frac{\epsilon}{2})[\frac{\partial\hat{u}^{n+1}}{\partial x}]^2_{x=x_k}+\sum_{k=0}^{N}\frac{\alpha}{2}[(\hat{u}^{n+1})^2\hat{v}^n]_{x=x_k}\\
&+\sum_{k=1}^{N}\int_{x_{k-1}}^{x_k}0.5\alpha(\hat{u}^{n+1})^2\frac{\partial\hat{v}^n}{\partial x}\,\mathrm{d}x-\sum_{k=1}^{N}\frac{\theta_1}{2}\|f_1^{n+1}\|^2_{\mathcal{L}^2(I_k)}-\sum_{k=1}^{N}\frac{\theta_1}{2}\|\hat{u}^{n+1}\|^2_{\mathcal{L}^2(I_k)}\le 0.
\end{aligned}
$$

Using the fact that $\frac{(a+b)^2}{2}\le(a^2+b^2)$ and the inequality (4.4) for the term R_8, we get

$$
\Big(\{\frac{\partial\hat{u}^{n+1}}{\partial x}\}|_{x=x_k}\Big)^2\le\frac{p^2+1}{h_e}\Big(\Big\|\frac{\partial\hat{u}^{n+1}}{\partial x}\Big\|^2_{\mathcal{L}^2(I_k)}+\Big\|\frac{\partial\hat{u}^{n+1}}{\partial x}\Big\|^2_{\mathcal{L}^2(I_{k+1})}\Big),
$$

therefore

$$
\sum_{k=1}^{N}\frac{1}{2\Delta t}(\|\hat{u}^{n+1}\|^2_{\mathcal{L}^2(I_k)}-\|\hat{u}^{n}\|^2_{\mathcal{L}^2(I_k)})+\epsilon\Big(\underbrace{1-\frac{\gamma_1}{h_e}(p^2+1)}_{R_9}\Big)\sum_{k=1}^{N}\Big\|\frac{\partial\hat{u}^{n+1}}{\partial x}\Big\|^2_{\mathcal{L}^2(I_k)}
$$

$$+\sum_{k=0}^{N}\underbrace{(\sigma_u-\frac{\epsilon}{2\gamma_1})}_{R_{10}}[\hat{u}^{n+1}]^2_{x=x_k}+\sum_{k=0}^{N}\underbrace{\frac{\eta}{3}[(\hat{u}^{n+1})^3]_{x=x_k}}_{R_{13}}-\frac{\epsilon}{2}\sum_{k=0}^{N}(\{\hat{u}^{n+1}\}|_{x=x_k})^2$$
$$+\sum_{k=0}^{N}\underbrace{(\sigma_{u_x}-\frac{\epsilon}{2})}_{R_{11}}[\frac{\partial\hat{u}^{n+1}}{\partial x}]^2_{x=x_k}+\sum_{k=0}^{N}\underbrace{\frac{\alpha}{2}[(\hat{u}^{n+1})^2\hat{v}^n]_{x=x_k}}_{R_{14}}+\sum_{k=1}^{N}\int_{x_{k-1}}^{x_k}\frac{\alpha}{2}(\hat{u}^{n+1})^2$$
$$\times\frac{\partial\hat{v}^n}{\partial x}\,\mathrm{d}x+\sum_{k=1}^{N}\frac{\theta_1}{2}\|f_1^{n+1}\|^2_{\mathcal{L}^2(I_k)}-\sum_{k=1}^{N}\frac{\theta_1}{2}\|\hat{u}^{n+1}\|^2_{\mathcal{L}^2(I_k)}\le 0. \tag{4.9}$$

By choosing

$$\gamma_1\le h_e/(p^2+1),\quad \sigma_u>\epsilon/(2\gamma_1),\quad \sigma_{u_x}>\epsilon/2, \tag{4.10}$$

terms R_9, R_{10} and R_{11} remain nonnegative. In the terms R_{13} and R_{14}, values $\eta\hat{u}^{n+1}(x_k)$ and $\alpha\hat{v}^n(x_k)$ may be positive or negative thus according to the definition of the jump, we have positive and negative parts. We only need to consider the negative parts to find a lower bond. Now, using positiveness of the terms R_9, R_{10} and R_{11}, the lower bound of (4.9) is obtained by

$$\sum_{k=1}^{N}\frac{1}{2\Delta t}(\|\hat{u}^{n+1}\|^2_{\mathcal{L}^2(I_k)}\le\|\hat{u}^{n}\|^2_{\mathcal{L}^2(I_k)})+\frac{\epsilon}{2}\sum_{k=0}^{N}\underbrace{(\hat{u}^{n+1}(x_k))^2}_{R_{15}}$$
$$+\frac{|\eta|}{3}(\max_{k=0,\dots,N}\hat{u}^{n+1}(x_k))\sum_{k=1}^{N}\underbrace{(\hat{u}^{n+1}(x_k))^2}_{R_{15}}+\frac{|\alpha|}{2}(\max_{k=0,\dots,N}\hat{v}^{n}(x_k))\sum_{k=1}^{N}\underbrace{(\hat{u}^{n+1}(x_k))^2}_{R_{15}}$$
$$-\sum_{k=1}^{N}\underbrace{\int_{x_{k-1}}^{x_k}\frac{\alpha}{2}(\hat{u}^{n+1})^2\frac{\partial\hat{v}^n}{\partial x}\,\mathrm{d}x}_{R_{12}}+\sum_{k=1}^{N}\frac{\theta_1}{2}\|f_1^{n+1}\|^2_{\mathcal{L}^2(I_k)}+\sum_{k=1}^{N}\frac{\theta_1}{2}\|\hat{u}^{n+1}\|^2_{\mathcal{L}^2(I_k)}.$$

For the term R_{12}, from the first mean value theorem for definite integrals, we have

$$\int_{x_{k-1}}^{x_k}\frac{\alpha}{2}(\hat{u}^{n+1})^2\frac{\partial\hat{v}^n}{\partial x}\,\mathrm{d}x=\frac{\alpha}{2}\|\hat{u}^{n+1}\|^2_{\mathcal{L}^2(I_k)}(\frac{\partial\hat{v}^n}{\partial x}|_{x=c\in[x_{k-1},x_k]}).$$

For the term R_{13}, from the inequality (4.3), we have

$$\sum_{k=1}^{N}\frac{1}{2\Delta t}(\|\hat{u}^{n+1}\|^2_{\mathcal{L}^2(I_k)}-\|\hat{u}^{n}\|^2_{\mathcal{L}^2(I_k)})\le\frac{\epsilon}{2h_e}(p+1)^2\sum_{k=1}^{N}\|\hat{u}^{n+1}\|^2_{\mathcal{L}^2(I_k)}$$
$$+\frac{|\eta|}{3h_e}\Big(\max_{k=0,\dots,N}\hat{u}^{n+1}(x_k)\Big)(p+1)^2\sum_{k=1}^{N}\|\hat{u}^{n+1}\|^2_{\mathcal{L}^2(I_k)}$$

$$+\frac{|\alpha|}{2h_e}\Big(\max_{k=0,\dots,N}\hat{v}^n(x_k)\Big)(p+1)^2\sum_{k=1}^{N}\|\hat{u}^{n+1}\|^2_{\mathcal{L}^2(I_k)}-\frac{|\alpha|}{2}\Big(\max_{x\in\Omega}\frac{\partial\hat{v}^n}{\partial x}\Big)$$
$$\times\sum_{k=1}^{N}\|\hat{u}^{n+1}\|^2_{\mathcal{L}^2(I_k)}+\sum_{k=1}^{N}\frac{\theta_1}{2}\|f_1^{n+1}\|^2_{\mathcal{L}^2(I_k)}+\sum_{k=1}^{N}\frac{\theta_1}{2}\|\hat{u}^{n+1}\|^2_{\mathcal{L}^2(I_k)}. \tag{4.11}$$

Thus, we can rewrite (4.11) as follows:

$$\begin{aligned}\sum_{k=1}^{N}(\|\hat{u}^{n+1}\|^2_{\mathcal{L}^2(I_k)}-\|\hat{u}^{n}\|^2_{\mathcal{L}^2(I_k)})&\le \Delta t C_1\sum_{k=1}^{N}\|\hat{u}^{n+1}\|^2_{\mathcal{L}^2(I_k)}\\&+\theta_1\Delta t\sum_{k=1}^{N}\|f_1^{n+1}\|^2_{\mathcal{L}^2(I_k)},\end{aligned} \tag{4.12}$$

where

$$\begin{aligned}C_1=&\frac{\epsilon}{h_e}(p+1)^2+\frac{2|\eta|}{3h_e}\Big(\max_{k=0,\dots,N}\hat{u}^{n+1}(x_k)\Big)(p+1)^2\\&+\frac{|\alpha|}{h_e}\Big(\max_{k=0,\dots,N}\hat{v}^{n}(x_k)\Big)(p+1)^2-|\alpha|\max_{x\in\Omega}\frac{\partial\hat{v}^n}{\partial x}+\theta_1.\end{aligned} \tag{4.13}$$

By summation of Equation (4.12) over n from 0 to $m-1$, we obtain

$$\begin{aligned}\sum_{k=1}^{N}\|\hat{u}^{m}\|^2_{\mathcal{L}^2(I_k)}\le&\sum_{k=1}^{N}\|\hat{u}^{0}\|^2_{\mathcal{L}^2(I_k)}+\Delta t C_1\sum_{n=1}^{m}\sum_{k=1}^{N}\|\hat{u}^{n}\|^2_{\mathcal{L}^2(I_k)}\\&+\theta_1\Delta t\sum_{n=1}^{m}\sum_{k=1}^{N}\|f_1\|^2_{\mathcal{L}^2(I_k)}.\end{aligned}$$

Thus, if $\Delta t < 1/C_1$, we can conclude the inequality (4.5) from the discrete Gronwall inequality. To obtain an acceptable range for Δt, one must consider the maximum value of C_1. Regarding the non-linearity of damping terms in the viscous coupled Burgers' equation [20], the behavior of the solution, which depends on the damping factor, would decay in time. Thus, the maximum value of $\hat{u}^{n+1}$ and $\hat{v}^n$ in (4.13) occurs at the initial time. In other words, C_1 can be computed as follows:

$$\begin{aligned}C_1=&\frac{\epsilon}{h_e}(p+1)^2+\frac{2|\eta|}{3h_e}\Big(\max_{k=0,\dots,N}\hat{u}^{0}(x_k)\Big)(p+1)^2\\&+\frac{|\alpha|}{h_e}\Big(\max_{k=0,\dots,N}\hat{v}^{0}(x_k)\Big)(p+1)^2-|\alpha|\max_{x\in\Omega}\frac{\partial\hat{v}^0}{\partial x}+\theta_1.\end{aligned}$$

□

5 Numerical results

We consider the following four examples to verify the IDG scheme for solving the coupled Burgers' equations. We show that the approximate solutions obtained using the IDG scheme are very close to the analytical solutions. We

define the relative error $\mathcal{L}^2_{error} = \frac{(\int_a^b |\hat{u}(x,t)-u^*(x,t)|^2\ dx)^{\frac{1}{2}}}{(\int_a^b |u^*(x,t)|^2\ dx)^{\frac{1}{2}}}$, where $\hat{u}(x,t)$ and $u^*(x,t)$ are approximate solution and analytical solution, respectively.

5.1 Example 1

If we take $\epsilon = 1,\ \eta = \xi = -2,\ \alpha = \beta = 1$ and $f_1 = f_2 = 0$ in Equation (2.1), we obtain the following viscous Burgers' equations in the region $-\pi \le x \le \pi$:

$$\begin{pmatrix} \frac{\partial u}{\partial t} \\ \frac{\partial v}{\partial t} \end{pmatrix} - \begin{pmatrix} \frac{\partial^2 u}{\partial x^2} \\ \frac{\partial^2 v}{\partial x^2} \end{pmatrix} + \begin{pmatrix} -2u+v & u \\ v & -2v+u \end{pmatrix} \begin{pmatrix} \frac{\partial u}{\partial x} \\ \frac{\partial v}{\partial x} \end{pmatrix} = \begin{pmatrix} 0 \\ 0 \end{pmatrix}, \quad t > 0,$$

with the initial conditions $u(x,0) = v(x,0) = \sin(x), \quad -\pi \le x \le \pi$, and the boundary conditions $u(\pm\pi,t) = v(\pm\pi,t) = 0$ for $t > 0$. The analytical solution for this problem expressed by [10] as $u^*(x,t) = v^*(x,t) = \exp(-t)\sin(x)$.

The approximate solutions, $\hat{v}(x,t)$, obtained by the IDG scheme (Case I) for different times, are shown in Figure 1. To obtain stable approximate solutions,

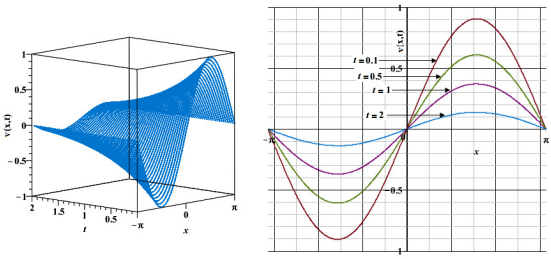

Figure 1. Approximate solutions $\hat{v}(x,t)$ by using the IDG scheme (Case I) for $t \in [0,2]$ and $-\pi \le x \le \pi$.

we use Theorem 2. By considering $\gamma_1 = 0.0005$ and from (4.10), we can choose $\sigma_u = \sigma_v = 1000$. In Table 1, the suitable range of the time step, Δt, from Theorem 2 for different degrees of polynomials and various N is obtained. The accuracy of the IDG scheme for Example 1 is demonstrated by the relative errors with different N and p in Table 2.

Table 1. Suitable range of time step, Δt, for the Example 1 using the IDG scheme.

	N				
p	4	8	16	32	64
1	0.2024	0.0919	0.0439	0.0215	0.0106
2	0.0808	0.0388	0.0191	0.0094	0.0047
3	0.0439	0.0215	0.0106	0.0053	0.0026

We compared the current work with the available results. Comparisons indicate that the errors in the IDG scheme are similar to the results of Srivastava et al. [23], which used the implicit logarithmic finite difference scheme with $\Delta t = 0.001$ and $N = 200$; Lai and Ma [15], that applied the lattice Boltzmann method with $\Delta t = 0.001$ and $N = 64$; Rashid and Ismail [21], that employed

Table 2. Relative errors for $\hat{v}(x,t)$ in Example 1 for $x \in [-\pi,\pi]$ and various T_f with $\Delta t = 0.001$, $\sigma_u = \sigma_v = 10^3$.

T_f	p	N = 4	8	16	32	64
0.1	1	1.26696 E-2	2.61533 E-3	6.26022 E-4	1.64988 E-4	6.44855 E-5
	2	1.81340 E-4	2.84257 E-4	6.04026 E-5	4.84588 E-5	4.81957 E-5
	3	1.85928 E-4	4.97455 E-5	4.81567 E-5	4.81665 E-5	4.80639 E-5
0.5	1	8.38453 E-2	1.78700 E-2	4.35475 E-3	1.16908 E-3	4.15725 E-4
	2	1.25705 E-2	1.77412 E-3	3.25369 E-4	2.31943 E-4	2.28687 E-4
	3	1.25715 E-3	2.41851 E-4	2.27490 E-4	2.27446 E-4	2.26833 E-4
1	1	2.51929 E-1	5.65252 E-2	1.39335 E-2	3.69656 E-3	1.19484 E-3
	2	3.44788 E-3	4.71472 E-3	7.77193 E-4	4.77557 E-4	4.64184 E-4
	3	3.36959 E-3	5.08605 E-4	4.58351 E-4	4.58057 E-4	4.56841 E-4

the Fourier pseudospectral method with $N = 64$ for the spatial discretization and the fourth-order Runge-Kutta method with $\Delta t = 0.0001$ for the time discretization; Mittal and Arora [17], that used the cubic B-spline collocation scheme with $\Delta t = 0.001$ and $N = 64$.

5.2 Example 2

Consider $\epsilon = 1$, $\eta = \xi = -2$, $\alpha = \beta = \frac{5}{2}$ and $f_1 = f_2 = 0$ in Equation (2.1). We have the following viscous Burgers' equations in the region $-20 \le x \le 20$, for $t > 0$, as

$$\begin{pmatrix} \frac{\partial u}{\partial t} \\ \frac{\partial v}{\partial t} \end{pmatrix} - \begin{pmatrix} \frac{\partial^2 u}{\partial x^2} \\ \frac{\partial^2 v}{\partial x^2} \end{pmatrix} + \begin{pmatrix} -2u + \frac{5}{2}v & \frac{5}{2}u \\ \frac{5}{2}v & -2v + \frac{5}{2}u \end{pmatrix} \begin{pmatrix} \frac{\partial u}{\partial x} \\ \frac{\partial v}{\partial x} \end{pmatrix} = \begin{pmatrix} 0 \\ 0 \end{pmatrix},$$

with the initial conditions $u(x,0) = v(x,0) = \lambda(1 - \tanh(\frac{3}{2}\lambda x))$, $-20 \le x \le 20$. The boundary conditions for this problem are extracted from the analytical solution given in [1].

The analytical solution for $-20 \le x \le 20$ and $t > 0$ is $u^*(x,t) = v^*(x,t) = \lambda\Big(1 - \tanh(\frac{3}{2}\lambda(x - 3\lambda t))\Big)$. The approximate solutions of $\hat{v}(x,t)$ for different times with the IDG scheme (Case I) are demonstrated in Figure 2.

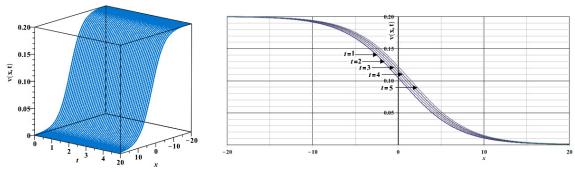

Figure 2. Approximate solutions, $\hat{v}(x,t)$, using the IDG scheme (Case I) for $t \in [0,5]$ and $-20 \le x \le 20$.

By using (4.10) and considering $\gamma_1 = 0.0005$, we get $\sigma_u = \sigma_v = 1000$. From Theorem 2, the suitable range of the time step, Δt, can be estimated for different p and various N (see Table 3).

Table 3. Suitable range of time step, Δt, for Example 2 using the IDG scheme.

	N		
p	5	20	50
1	1.3567	0.3415	0.1368
2	0.6061	0.1520	0.0608
3	0.3415	0.0855	0.0342

Using the IDG scheme with $\Delta t = 0.01$, $N = 50$, and $p = 3$, we get similar relative errors to [15] that used the lattice Boltzmann method and the finite difference with $\Delta t = 0.001$ and $N = 320$. The relative errors using the IDG scheme with $\Delta t = 0.01$, $N = 50$, and $p = 3$ are little more than the relative errors obtained by Bak et al. [4] using the backward semi-Lagrangian scheme with $\Delta t = 0.1$ and $N = 640$. In Table 4, the accuracy of the IDG scheme (for Case I) is shown.

Table 4. Relative errors for $\hat{v}(x,t)$ in Example 2 for $x \in [-20, 20]$ and various T_f with $\Delta t = 0.01$, $\sigma_u = \sigma_v = 10^3$ and $\lambda = 0.1$.

		N		
T_f	p	5	20	50
1	1	2.90969 E-3	1.10012 E-4	7.82797 E-5
	2	1.37085 E-4	9.21670 E-6	3.20660 E-6
	3	1.19795 E-5	3.22988 E-6	3.15304 E-6 1
2	1	8.51364 E-2	2.00530 E-4	2.97094 E-5
	2	1.26148 E-2	1.81712 E-5	5.88707 E-6
	3	1.27034 E-3	5.92573 E-6	5.77084 E-6
5	1	1.36445 E-2	5.17610 E-4	7.82797 E-5
	2	8.99441 E-4	4.32790 E-5	1.21563 E-6
	3	5.59876 E-4	1.21945 E-5	1.18190 E-6

5.3 Example 3

We test the IEDG scheme to Equations (2.1) with $\epsilon = 10^{-l}$, $l = 1, 2$, $\eta = -\xi = 2$, and $\alpha = -\beta = 1$. The Dirichlet boundary conditions are homogeneous, and the initial conditions are:

$$u(x,0) = \begin{cases} \sin(2\pi x), & 0 \le x \le 0.5 \\ 0, & 0.5 \le x \le 1 \end{cases}, \qquad v(x,0) = \begin{cases} 0, & 0 \le x \le 0.5 \\ \sin(2\pi x), & 0.5 \le x \le 1 \end{cases}.$$

To show that the IEDG scheme (Case II) is a robust approximate solution for solving the coupled singularly perturbed Burgers' equations, we compared the IEDG scheme with a robust economic scheme [19] with $\epsilon = 10^{-l}$, $l = 1, 2$ for $t = 0.2, 0.4, 0.6, 0.8, 1$. Park et al. [19] discretized Equations (2.1) using the third-order backward differentiation formula for the material derivative, the standard fourth-order finite difference for the diffusion, and the fourth-order compact finite difference for the first spatial derivative. We obtained similar results for $\epsilon = 0.1$, except that they considered $\Delta t = 0.02$, $N = 50$, while we

considered $\Delta t = 0.04$, $N = 20$. In Figure 3, we demonstrated the IEDG scheme $\epsilon = 0.1$ with $\Delta t = 0.04$, $N = 20$, $\sigma_u = \sigma_v = 10^5$ and $\sigma_{u_x} = \sigma_{v_x} = 10^3$, and $p = 2$. Also, using the IEDG scheme with $\Delta t = 0.02$, $N = 50$, and $p = 2$, we get similar results to [19] that used economical robust method with $\Delta t = 0.0025$ and $N = 400$. We show the approximate solutions of $\hat{u}(x,t)$ and $\hat{v}(x,t)$ for different times with the IEDG scheme for $\epsilon = 0.01$, $\Delta t = 0.02$, $N = 50$, and $p = 2$ in Figure 4.

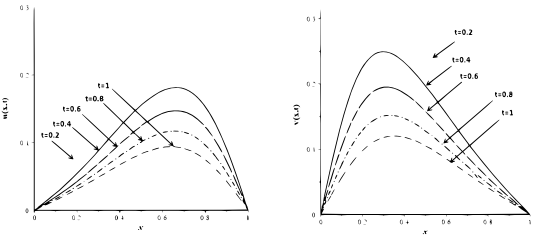

Figure 3. Approximate solutions $u(x,t)$ (left) and $v(x,t)$ (right) for Example 3, using the IEDG scheme (Case II) for $\epsilon = 0.1$, $\eta = -\xi = 2$, and $\alpha = -\beta = 1$ at $t = 0.2, 0.4, 0.6, 0.8, 1$ and $0 \le x \le 1$ with $N = 20$, $p = 2$, $\Delta t = 0.04$, $\sigma_u = \sigma_v = 10^5$ and $\sigma_{u_x} = \sigma_{v_x} = 10^3$.

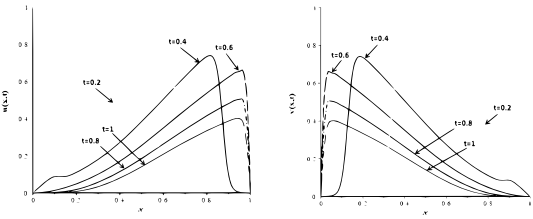

Figure 4. Approximate solutions $u(x,t)$ (left) and $v(x,t)$ (right) for Example 3, using the IEDG scheme (Case II) for $\epsilon = 0.01$, $\eta = -\xi = 2$, and $\alpha = -\beta = 1$ at $t = 0.2, 0.4, 0.6, 0.8, 1$ and $0 \le x \le 1$ with $N = 50$, $p = 2$, $\Delta t = 0.02$, $\sigma_u = \sigma_v = 10^5$ and $\sigma_{u_x} = \sigma_{v_x} = 10^3$.

This example has been solved by the finite difference method in [6], with the difference that $\epsilon = 1$ and by increasing the values of α and β, the effect of increasing the Reynolds number has been investigated.

5.4 Example 4

In the last test example, we employ the IEDG scheme to Equation (2.1) with $\epsilon = 10^{-l}$, $l = 3, 4, 5$, $\eta = \xi = 1$, and $\alpha = \beta = 1$. The Dirichlet boundary conditions, initial conditions, and the functions f_1 and f_2 are chosen so that the exact solutions are: $u^*(x,t) = -2v^*(x,t)$, $v^*(x,t) = -\tanh\left(\frac{x}{2\epsilon}\right)\exp(-\epsilon t)$. In the previous two test examples, we only reported the results obtained by Case I since there was not much difference between the numerical results obtained by Case I and Case II. In this example, we intend to show that the IEDG scheme (Case II) yields a robust approximate solution for solving the coupled singularly perturbed Burgers' equations. Thus we find the approximate solution of this example using both IDG (Case I) and IEDG (Case II) schemes with

$\epsilon = 10^{-l},\ l = 3, 4, 5$ for $t = 0.1$ and $t = 0.2$. The suitable range of the Δt for different p with $N = 21$ in Case II using Theorem 2, are presented in Table 5. In Figure 5, logarithm (base 10) of absolute errors between the exact solution,

Table 5. Suitable range of time step, Δt, for Example 3 using the IEDG scheme.

	ϵ		
p	0.001	0.0001	0.00001
1	0.009995801763	0.009999580018	0.009999958000
2	0.004492473983	0.004494191146	0.004494362934
3	0.002536989304	0.002537962848	0.002538060244

$u^*(x,t)$ and approximate solutions, $\hat{u}(x,t)$, with $N = 21$, $p = 2$, $\Delta t = 0.002$, $\sigma_u = 100$ and $\sigma_{u_x} = 1$ of two cases are demonstrated for $\epsilon = 10^{-l},\ l = 3, 4, 5$ at $t = 0.1$. As seen in these figures at $t = 0.1$, log-absolute errors of Case II are

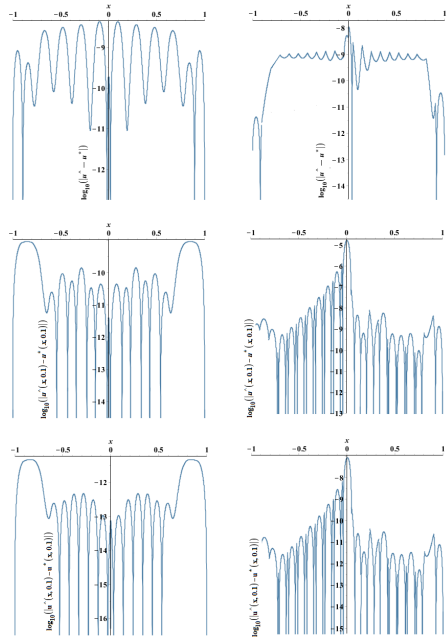

Figure 5. Plot of the logarithm (base 10) of the absolute error between the approximate solution, $\hat{u}(x,t)$, and exact solution, $u^*(x,t)$, for Example 3 at $T_f = 0.1$ with $N = 21$, $p = 2$, $\Delta t = 0.002$, $\sigma_u = 100$ and $\sigma_{u_x} = 1$ using the IDG scheme (left column) and the IEDG scheme (right column): first row for $\epsilon = 10^{-3}$, second row for $\epsilon = 10^{-4}$, and the last row for $\epsilon = 10^{-5}$.

smaller than Case I. But after passing the time (t=0.2), Case II (IEDG scheme) has log-absolute errors much more than Case I (IDG scheme) (see Figure 6). In other words, log-absolute errors at $t = 0.2$ are increased compared to log-absolute errors at $t = 0.1$ in Case I, whereas in Case II, log-absolute errors do not change much when the time is marched. Comparisons between the exact and approximate solutions obtained from both cases are shown in Figure 7 at $t = 0.2$.

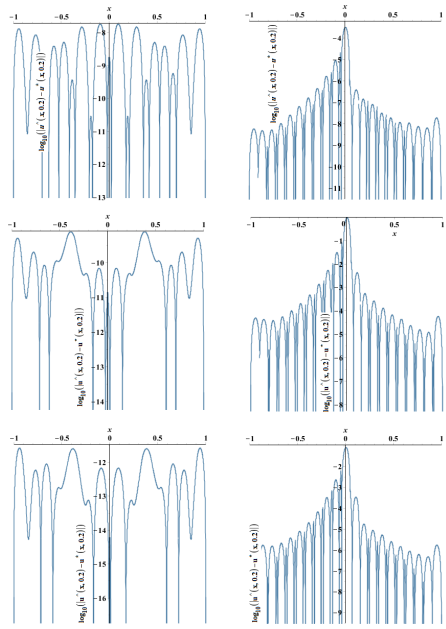

Figure 6. Plot of the logarithm (base 10) of the absolute error between the approximate solution, $\hat{u}(x,t)$, and exact solution, $u^*(x,t)$, for Example 3 at $T_f = 0.2$ with $N = 21$, $p = 2$, $\Delta t = 0.002$, $\sigma_u = 100$ and $\sigma_{u_x} = 1$ using the IDG scheme (left column) and the IEDG scheme (right column): first row for $\epsilon = 10^{-3}$, second row for $\epsilon = 10^{-4}$, and the last row for $\epsilon = 10^{-5}$.

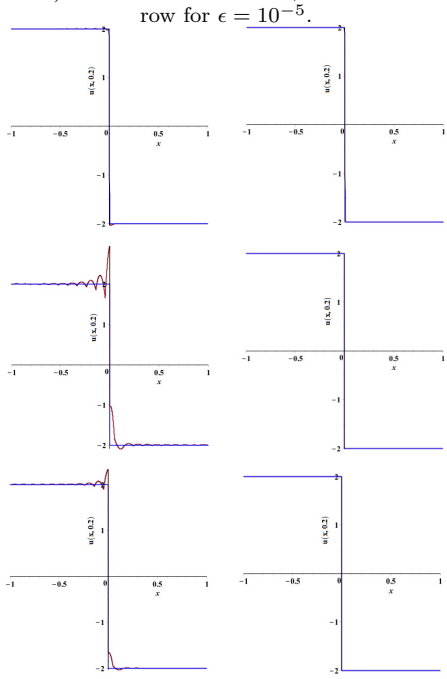

Figure 7. Comparison of the approximate solution, $\hat{u}(x, 0.2)$ for Example 3 with $N = 21$, $p = 2$, $\Delta t = 0.002$, $\sigma_u = 100$ and $\sigma_{u_x} = 1$, left column by using the IDG scheme and right column by using the IEDG scheme: first row for $\epsilon = 10^{-3}$, second row for $\epsilon = 10^{-4}$, and the last row for $\epsilon = 10^{-5}$.

For $\epsilon = 10^{-l},\ l = 3, 4, 5$, this example has a large Peclet number; thus, the probability of occurrence of overshoot and undershoot phenomena in numerical results increases. As shown in the left column of Figure 7, these phenomena appear in approximate solutions by Case I at $t = 0.2$. At the same time, no effect of phenomena is observed in approximate solutions obtained by Case II (see the right column of Figure 7). These results show the efficiency of the IEDG scheme.

6 Conclusions

In this paper, we presented IDG and IEDG schemes. These schemes provided numerical solutions for the coupled viscous and singularly perturbed Burgers' equations. The schemes employ the modal discontinuous Galerkin and Backward Euler methods for spatial and temporal discretization, respectively. To show the efficiency of the IEDG scheme, we increased the Peclet number by considering a small diffusion term, which leads to overshoot and undershoot phenomena in most of the approximate solutions. By using slope limiters, the phenomena are reduced. We apply the IEDG scheme to overcome overshoot and undershoot phenomena without using slope limiters.We obtained acceptable penalty terms and time step ranges using the stability analysis. Also, we computed the constant of the trace inequality for the approximate function and its first derivatives based on Legendre basis functions in the context of stability analysis. The four test examples demonstrate the applicability and effectiveness of the proposed schemes. The numerical comparisons indicate that there is a good agreement between the numerical solutions and exact solutions. Also, good results were obtained for the problems that do not have exact solutions compared to the available literature. We can easily generalize the scheme for the two-dimensional space with large Reynolds numbers. However, if there is a singularity, the equation becomes similar to the hyperbolic equation, and it is necessary to apply a suitable limiter. While in one-dimensional space, despite the singularity, there is no need to use any limiter.

References

[1] R. Abazari and A. Borhanifar. Numerical study of the solution of the Burgers and coupled Burgers equations by a differential transformation method. *Comput. Math. Appl.*, **59**(8):2711–2722, 2010. https://doi.org/10.1016/j.camwa.2010.01.039.

[2] A.A. Alderremy, S. Saleem and F.A. Hendi. A comparative analysis for the solution of nonlinear Burgers' equation. *J Integr Neurosci.*, **14**(3-4):503–523, 2018. https://doi.org/10.3233/JIN-180085.

[3] M. Baccouch and S. Kaddeche. Efficient Chebyshev pseudospectral methods for viscous Burgers' equations in one and two space dimensions. *Int. j. appl. math. comput.*, **5**(1):18, 2019. https://doi.org/10.1007/s40819-019-0602-6.

[4] S. Bak, P. Kim and D. Kim. A semi-Lagrangian approach for numerical simulation of coupled Burgers' equations. *Commun Nonlinear Sci Numer Simul.*, **69**:31–44, 2019. https://doi.org/10.1016/j.cnsns.2018.09.007.

[5] H.O. Bakodah, N.A. Al-Zaid, M. Mirzazadeh and Q. Zhou. Decomposition method for solving Burgers' equation with Dirichlet and Neumann boundary conditions. *Optik.*, **130**:1339–1346, 2017. https://doi.org/10.1016/j.ijleo.2016.11.140.

[6] A. Bashan. A numerical treatment of the coupled viscous Burgers' equation in the presence of very large Reynolds number. *Physica A: Statistical Mechanics and its Applications*, **545**:123755, 2020. https://doi.org/10.1016/j.physa.2019.123755.

[7] M. Bause and K. Schwegler. Higher order finite element approximation of systems of convection-diffusion-reaction equations with small diffusion. *J. Comput. Appl. Math.*, **246**:52–64, 2013. https://doi.org/10.1016/j.cam.2012.07.005.

[8] E.H. Doha, A.H. Bhrawy, M.A. Abdelkawy and R.M. Hafez. A Jacobi collocation approximation for nonlinear coupled viscous Burgers' equation. *Eur. J. Phys.*, **12**(2):111–122, 2014. https://doi.org/10.2478/s11534-014-0429-z.

[9] S. Gowrisankar and S. Natesan. An efficient robust numerical method for singularly perturbed Burgers' equation. *Appl. Math. Comput.*, **346**:385–394, 2019. https://doi.org/10.1016/j.amc.2018.10.049.

[10] D. Kayao. An explicit solution of coupled viscous Burgers' equation by the decomposition method. *International Journal of Mathematics and Mathematical Sciences*, **27**(11):675–680, 2001. https://doi.org/10.1155/S0161171201010249.

[11] A.H. Khater, R.S. Temsah and M.M. Hassan. A Chebyshev spectral collocation method for solving Burgers'-type equations. *J. Comput. Appl. Math.*, **222**(2):333–350, 2008. https://doi.org/10.1016/j.cam.2007.11.007.

[12] S. Khodayari-Samghabadi and S.H. Momeni-Masuleh. Implicit-modal discontinuous Galerkin scheme for two-phase flow with discontinuous capillary pressure. *SIAM J. Sci. Comput.*, **40**(4):B1131–B1160, 2018. https://doi.org/10.1137/17M1119937.

[13] M. Klinge and R. Weiner. Strong stability preserving explicit peer methods for discontinuous Galerkin discretizations. *J. Sci. Comput.*, **75**(2):1057–1078, 2018. https://doi.org/10.1007/s10915-017-0573-x.

[14] J.G.L. Laforgue and R.E. O'Malley Jr. Exponential asymptotics, the viscid Burgers' equation, and standing wave solutions for a reaction-advection-diffusion model. *Stud. Appl. Math.*, **102**(2):137–172, 1999. https://doi.org/10.1111/1467-9590.00107.

[15] H. Lai and C. Ma. A new lattice Boltzmann model for solving the coupled viscous Burgers' equation. *Physica A Stat. Mech.*, **395**:445–457, 2014. https://doi.org/10.1016/j.physa.2013.10.030.

[16] Q. Li, Z. Chai and B. Shi. A novel lattice Boltzmann model for the coupled viscous Burgers' equations. *Appl. Math. Comput.*, **250**:948–957, 2015. https://doi.org/10.1016/j.amc.2014.11.036.

[17] R.C. Mittal and G. Arora. Numerical solution of the coupled viscous Burgers' equation. *Commun. Nonlinear Sci. Numer. Simulat.*, **16**(3):1304–1313, 2011. https://doi.org/10.1016/j.cnsns.2010.06.028.

[18] R.C. Mittal and R. Jiwari. A differential quadrature method for numerical solutions of Burgers'-type equations. *Int. J. Numer. Methods Heat Fluid Flow*, **22**(7):880–895, 2012. https://doi.org/10.1108/09615531211255761.

[19] S. Park, P. Kim, Y.Jeon and S. Bak. An economical robust algorithm for solving 1D coupled Burgers' equations in a semi-Lagrangian

framework. *Applied Mathematics and Computation*, **428**:127185, 2022. https://doi.org/10.1016/j.amc.2022.127185.

[20] C.S. Rao, P.L. Sachdev and M. Ramaswamy. Self-similar solutions of a generalized Burgers equation with nonlinear damping. *Nonlinear Anal. Real World Appl.*, **4**(5):723–741, 2003. https://doi.org/10.1016/S1468-1218(02)00083-4.

[21] A. Rashid and A.I.B. Ismail. A Fourier pseudospectral method for solving coupled viscous Burgers equations. *Int. J. Comput. Methods*, **9**(4):412–420, 2009. https://doi.org/10.2478/cmam-2009-0026.

[22] B.D. Reddy. *Introductory functional analysis: with applications to boundary value problems and finite elements*, volume 27. Springer Science & Business Media, 1991.

[23] V.K. Srivastava, M. Tamsir, M.K. Awasthi and S. Singh. One-dimensional coupled Burgers' equation and its numerical solution by an implicit logarithmic finite-difference method. *AIP Adv.*, **4**(3):037119, 2014. https://doi.org/10.1063/1.4869637.

[24] B. Tripathi, A. Luca, S. Baskar, F. Coulouvrat and R. Marchiano. Element centered smooth artificial viscosity in discontinuous Galerkin method for propagation of acoustic shock waves on unstructured meshes. *J. Comput. Phys.*, **366**:298–319, 2018. https://doi.org/10.1016/j.jcp.2018.04.010.

[25] M. Uzunca. *Adaptive discontinuous Galerkin methods for non-linear reactive flows*. Springer, 2016. https://doi.org/10.1007/978-3-319-30130-3.

[26] T. Warburton and J.S. Hesthaven. On the constants in *hp*-finite element trace inverse inequalities. *Comput. Methods in Appl. Mech. Eng.*, **192**(25):2765–2773, 2003. https://doi.org/10.1016/S0045-7825(03)00294-9.